

*Supporting Information for*

**Narrower Nanoribbon Biosensors  
Fabricated by Chemical Lift-Off Lithography  
Show Higher Sensitivity**

Chuanzhen Zhao,<sup>†,§</sup> Qingzhou Liu,<sup>□</sup> Kevin M. Cheung,<sup>†,§</sup> Wenfei Liu,<sup>†,§</sup> Qing Yang,<sup>†,§</sup>  
Xiaobin Xu,<sup>†,§</sup> Tianxing Man,<sup>¶</sup> Paul S. Weiss<sup>†,§,▲,▼,\*</sup> Chongwu Zhou,<sup>□,#,\*</sup> and

Anne M. Andrews,<sup>†,§,▽,\*</sup>

<sup>†</sup>Department of Chemistry and Biochemistry, University of California, Los Angeles, Los Angeles, California 90095, United States

<sup>§</sup>California NanoSystems Institute, University of California, Los Angeles, Los Angeles, California 90095, United States

<sup>□</sup>Mork Family Department of Chemical Engineering and Materials Science, University of Southern California, Los Angeles, California 90089, United States

<sup>¶</sup>Department of Mechanical and Aerospace Engineering, University of California, Los Angeles, Los Angeles, California 90095, United States

<sup>▲</sup>Department of Bioengineering, University of California, Los Angeles, Los Angeles, California 90095, United States

<sup>▼</sup>Department of Materials Science and Engineering, University of California, Los Angeles, Los Angeles, California 90095, United States

<sup>#</sup>Ming Hsieh Department of Electrical Engineering, University of Southern California, Los Angeles, California 90089, United States

<sup>▽</sup>Department of Psychiatry and Biobehavioral Sciences, Semel Institute for Neuroscience and Human Behavior, and Hatos Center for Neuropharmacology, University of California, Los Angeles, Los Angeles, California 90095, United States

\*Address correspondence to aandrews@mednet.ucla.edu (AMA), chongwuz@usc.edu (CZ), and psw@cnsi.ucla.edu (PSW)

## Supplemental Methods

Artificial cerebrospinal fluid (aCSF) was prepared from stock solutions. The 10× base stock contains NaCl (1470 mM), KCl (35 mM), NaH<sub>2</sub>PO<sub>4</sub> (10 mM), and NaHCO<sub>3</sub> (25 mM) in deionized distilled water. The base stock is aliquoted and stored at room temperature. It is stable for at least one year. **Preparation note:** Neither CaCl<sub>2</sub> nor MgCl<sub>2</sub> should be added directly to the 10× base stock solution due to their low solubility in aqueous solution at pH >7.5. The Mg<sup>2+</sup> and Ca<sup>2+</sup> precipitate as Mg(OH)<sub>2</sub> and Ca(OH)<sub>2</sub> causing the stock solution to appear cloudy and/or for a visible precipitate to form. Stock solutions of CaCl<sub>2</sub> (901 mM) and MgCl<sub>2</sub> (1050 mM) in deionized distilled water are each prepared separately. **Safety note:** The addition of CaCl<sub>2</sub> or MgCl<sub>2</sub> to water is exothermic. Use caution, cold water, and slow stirring when preparing these solutions. The CaCl<sub>2</sub> and MgCl<sub>2</sub> stocks are aliquoted into 1-mL Eppendorf tubes and stored at -80 °C indefinitely.

Before experiments, the working aCSF solution (physiological concentration, “1×”) was prepared. One aliquot each of the CaCl<sub>2</sub> and MgCl<sub>2</sub> stocks was thawed. Deionized distilled water was added to a beaker at ~80% of the final volume of the working solution. The 10× base stock was added, *e.g.*, 50 mL 10× base stock was added to ~400 mL water for 500 mL final volume of working solution. The pH was initially adjusted to 7.4-7.5 with ~1% HCl. The CaCl<sub>2</sub> stock was then added dropwise slowly using a pipette. The working solution was constantly stirred to avoid precipitation for a final concentration of 1.0 mM CaCl<sub>2</sub>, *e.g.*, 555 μL for a final volume of 500 mL working solution. Next, the MgCl<sub>2</sub> stock solution was added dropwise slowly while stirring, for a final concentration of 1.2 mM, *e.g.*, 571 μL for a final volume of 500 mL working solution. The pH

of the working solution was adjusted to  $7.30 \pm 0.03$  using  $\sim 1\%$  HCl. Finally, the solution was brought to the final volume with deionized distilled water, *e.g.*, final volume 500 mL. The final concentrations of the working aCSF solution (1 $\times$ ) were NaCl (147 mM), KCl (3.5 mM), NaH<sub>2</sub>PO<sub>4</sub> (1.0 mM), NaHCO<sub>3</sub> (2.5 mM), CaCl<sub>2</sub> (1.0 mM), and MgCl<sub>2</sub> (1.2 mM). The working solution was stored at 4 °C for  $\leq 2$  weeks.

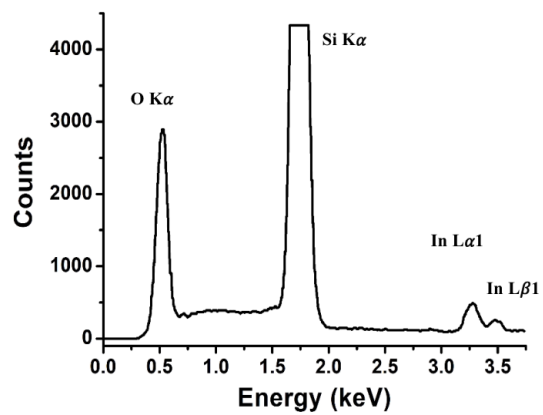


**Figure S1.** Elemental energy spectrum for  $\text{In}_2\text{O}_3$  nanoribbons from energy-dispersive X-ray mapping.

**Table S1.** Elemental quantification analysis of In<sub>2</sub>O<sub>3</sub> nanoribbons by energy-dispersive X-ray mapping.

<b>Element Line</b>	<b>Net Counts</b>	<b>Element wt.%</b>	<b>Element wt.% Error</b>	<b>Atom%</b>	<b>Atom% Error</b>
O K	26915	50.60	---	66.48	±0.51
Si L	0	---	---	---	---
Si K	213374	43.30	±0.14	32.40	±0.11
In M	0	---	---	---	---
In L	10378	6.10	±0.26	1.12	±0.05
Total		100.0		100.0	

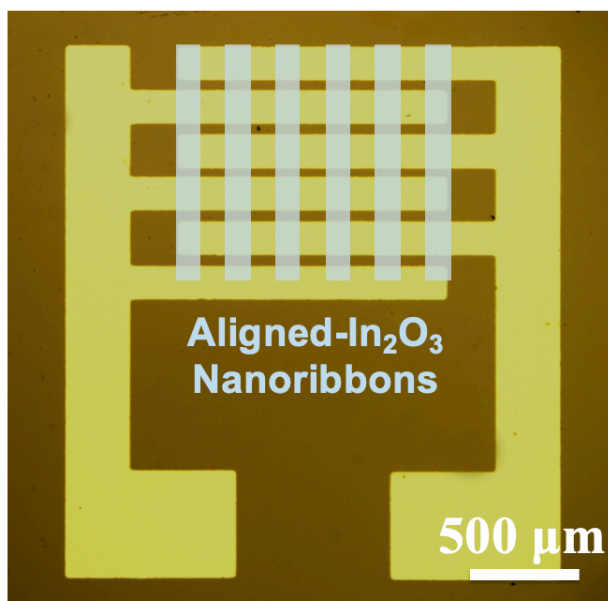


**Figure S2.** Optical microscope image of interdigitated electrodes (yellow). Orientations of In<sub>2</sub>O<sub>3</sub> nanoribbons are depicted in overlay (light blue).

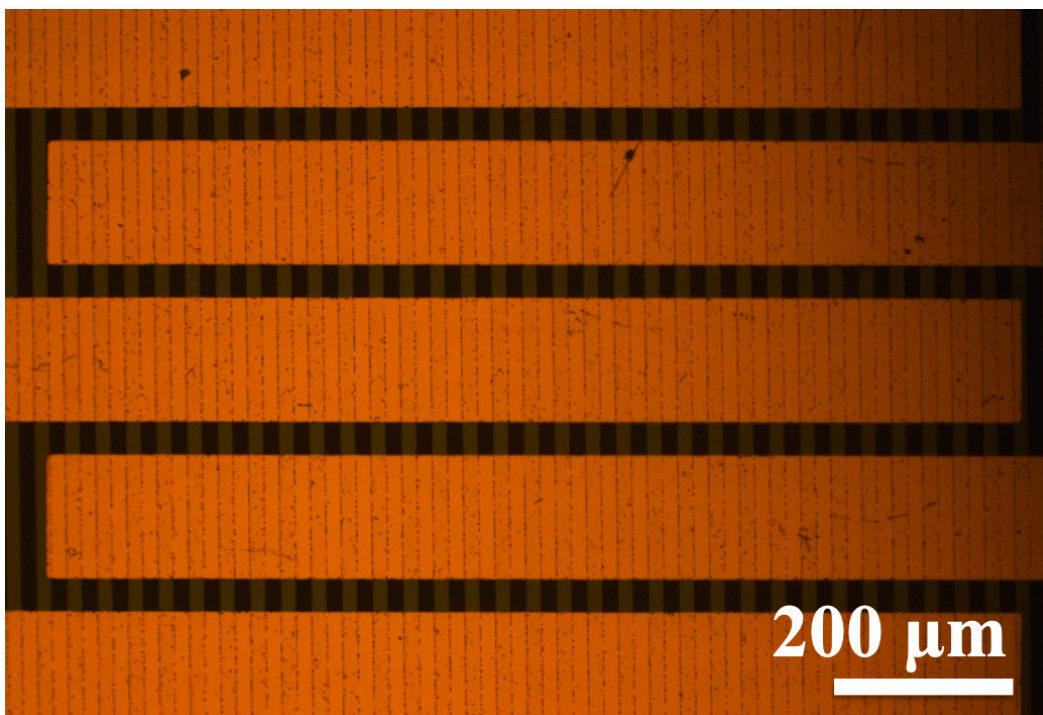


**Figure S3.** Optical microscope image of 20- $\mu\text{m}$  wide  $\text{In}_2\text{O}_3$  nanoribbons with source and drain electrodes.

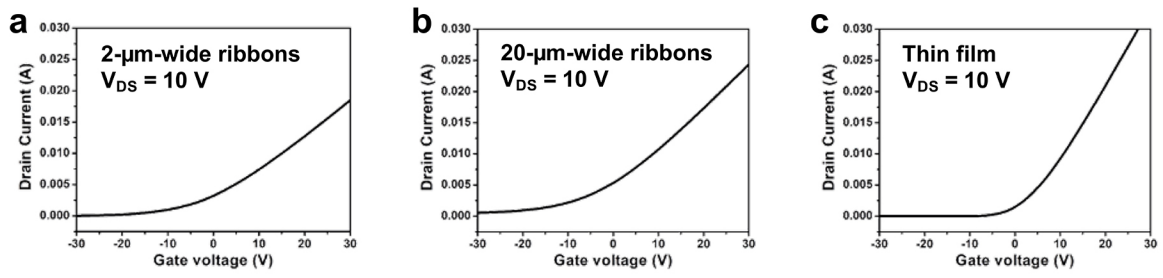


**Figure S4.** Solid-state transfer characteristics of  $\text{In}_2\text{O}_3$  FETs with different nanoribbon widths, **(a)** 2  $\mu\text{m}$ , **(b)** 20  $\mu\text{m}$ , and **(c)** thin film.



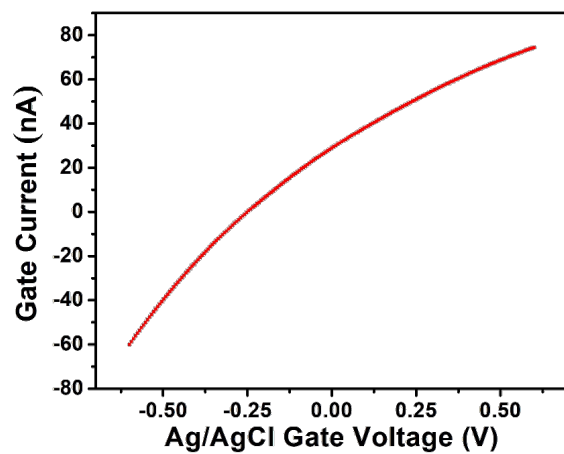


**Figure S5.** Gate leakage current (gate current to gate voltage) in buffer solution (pH = 7.4) at  $V_{DS} = 100$  mV.

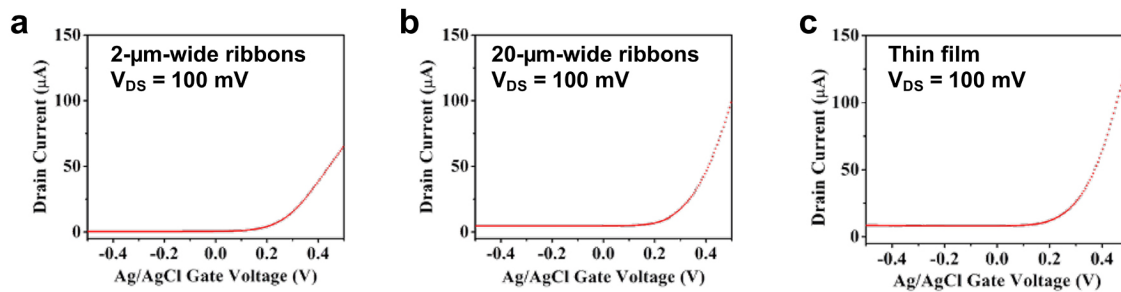


**Figure S6.** Liquid-state transfer characteristics of  $\text{In}_2\text{O}_3$  FETs with nanoribbons of different widths, **(a)** 2  $\mu\text{m}$ , **(b)** 20  $\mu\text{m}$ , or **(c)** thin film.

## Calculation of surface-to-volume ratios

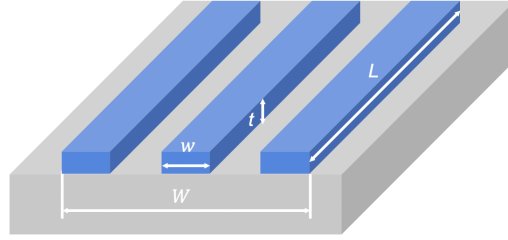


**Figure S7.** Schematic of nanoribbons for calculation of surface-to-volume ratios.

Consider a nanoribbon array, where the surface-to-volume ratio of an arbitrary area with width  $W$  is calculated. For each  $\text{In}_2\text{O}_3$  nanoribbon, the length is denoted as  $L$ , width as  $w$ , and thickness as  $t$ . The pitch of the nanoribbons is  $2w$  for different widths of nanoribbons. For nanoribbon surface area calculations, only the top surface and the two side surfaces are included. Results are summarized in **Table S2**.

$$\text{Number of ribbons (per arbitrary area): } N = \frac{W}{2w} \quad \text{Eq. 1}$$

$$\text{Surface area: } S = (w * L) + (2 * L * t) \quad \text{Eq. 2}$$

$$\text{Volume: } V = w * L * t \quad \text{Eq. 3}$$

$$\text{Surface-to-volume ratio (per nanoribbon): } \frac{S}{V} = \frac{w*L+2*L*t}{w*L*t} = \frac{w+2*t}{w*t} = \frac{1+2*\frac{t}{w}}{t} \quad \text{Eq. 4}$$

$$\text{Surface-to-volume ratio (per arbitrary area): } \frac{S}{V} = \frac{(w*L+2*L*t)*N}{(w*L*t)*N} = \frac{(w*L+2*L*t)}{(w*L*t)} = \frac{1+2*\frac{t}{w}}{t} \quad \text{Eq. 5}$$

For  $w_1 = 350 \text{ nm}$ :

$$\frac{S}{V} = \frac{1+2*\frac{t}{w}}{t} = \frac{1+2*\frac{20 \text{ nm}}{350 \text{ nm}}}{20 \text{ nm}} = \frac{1+0.11}{20} \text{ nm}^{-1} = \frac{1.11}{20} \text{ nm}^{-1}$$

For  $w_2 = 2 \mu\text{m}$ :

$$\frac{S}{V} = \frac{1+2*\frac{t}{w}}{t} = \frac{1+2*\frac{20 \text{ nm}}{2000 \text{ nm}}}{20 \text{ nm}} = \frac{1+0.02}{20} \text{ nm}^{-1} = \frac{1.02}{20} \text{ nm}^{-1}$$

For  $w_3 = 20 \mu\text{m}$ :

$$\frac{S}{V} = \frac{1+2*\frac{t}{w}}{t} = \frac{1+2*\frac{20 \text{ nm}}{20000 \text{ nm}}}{20 \text{ nm}} = \frac{1+0.002}{20} \text{ nm}^{-1} = \frac{1.002}{20} \text{ nm}^{-1}$$

For thin-films:

$$\frac{t}{w} \rightarrow 0, \frac{S}{V} = \frac{1+2*\frac{t}{w}}{t} = \frac{1}{20} \text{ nm}^{-1}$$

**Table S2.** Surface-to-volume ratios calculated for different configurations of In<sub>2</sub>O<sub>3</sub> FETs

<b>Width</b>	<b>Pitch</b>	<b>Thickness</b>	<b>Surface-to-Volume Ratio</b>	<b>Surface-to-Volume Ratio Increase vs Thin Film</b>
350 nm	700 nm	20 nm	$\frac{1.11}{20} \text{ nm}^{-1}$	11%
2 $\mu\text{m}$	4 $\mu\text{m}$	20 nm	$\frac{1.02}{20} \text{ nm}^{-1}$	2%
20 $\mu\text{m}$	40 $\mu\text{m}$	20 nm	$\frac{1.002}{20} \text{ nm}^{-1}$	0.2%
Thin Film	—	20 nm	$\frac{1}{20} \text{ nm}^{-1}$	—

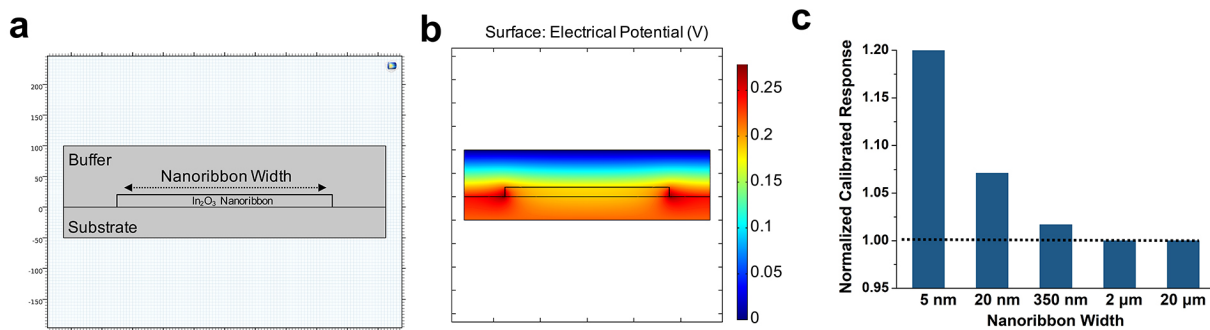


**Figure S8.** COMSOL simulations of effects of nanoribbon width on surface-to-volume ratio.

(a) Model used in the simulation, where nanoribbons are 20-nm-thick with widths varying from 5 nm to 20 μm. (b) Simulation results of the electrostatic potential due to the charge of the biomolecules. (c) Simulated normalized calibrated responses at different ribbon widths showing that the sensitivity of In<sub>2</sub>O<sub>3</sub> nanoribbon FETs is predicted to increase at widths below 2 μm. Simulated calibrated response values were normalized to responses for 20-μm microribbons. Simulated responses are not directly comparable with experimental results in the main text due to the nature of the simulation complexity for the semiconductor system under study.

**Table S3.** Field-effect transistor data were analyzed by two-way analysis of variance with nanoribbon width and target concentration as the independent variables.

Type	Figure	Interaction Term	Nanoribbon Width	Concentration
pH	Fig. 4f	F (5,24) = 3.395 <i>P</i> = 0.019	F (1,24) = 13.09 <i>P</i> = 0.001	F (5,24) = 307.0 <i>P</i> < 0.0001
Serotonin	Fig. 5c	F (5,18) = 0.375 <i>P</i> = 0.859	F (1,18) = 4.010 <i>P</i> = 0.061	F (5,18) = 9.107 <i>P</i> = 0.0002
DNA	Fig. 5f	F (3,10) = 0.054 <i>P</i> = 0.982	F (1,10) = 7.293 <i>P</i> = 0.022	F (3,10) = 1.518 <i>P</i> = 0.269